

ORIGINAL RESEARCH PAPER

## Van der Waals corrected DFT study on the adsorption behaviors of TiO<sub>2</sub> anatase nanoparticles as potential molecule sensor for thiophene detection

Amirali Abbasi<sup>1,2,3\*</sup>, Jaber Jahanbin Sardroodi<sup>1,2,3</sup>

<sup>1</sup> Molecular Simulation Laboratory (MSL), Azarbaijan Shahid Madani University, Tabriz, Iran

<sup>2</sup> Department of Chemistry, Faculty of Basic Sciences, Azarbaijan Shahid Madani University, Tabriz, Iran

<sup>3</sup> Computational Nanomaterials Research Group (CNRG), Azarbaijan Shahid Madani University, Tabriz, Iran

Received: 2016.08.29

Accepted: 2016.10.19

Published: 2017.01.30

### ABSTRACT

Density functional theory investigations were conducted in order to study the effects of the adsorption of thiophene on the structural and electronic properties of TiO<sub>2</sub> anatase nanoparticles. The ability of pristine and N-doped TiO<sub>2</sub> anatase nanoparticles to recognize toxic thiophene was surveyed in detail. It was found that thiophene molecule is chemisorbed on the N-doped anatase nanoparticles in S site geometries with large adsorption energy and small distance. By including van der Waals (vdW) interactions between thiophene molecule and TiO<sub>2</sub>, we found that the adsorption on the N-doped TiO<sub>2</sub> is energetically more favorable than the adsorption on the pristine one, suggesting that the nitrogen doping can energetically facilitate the thiophene adsorption on the N-doped nanoparticle. The order of adsorption energy is Parallel(S site)>Perpendicular(S site)>Perpendicular (H site). The interaction between thiophene and N-doped TiO<sub>2</sub> can induce substantial variations in the HOMO/LUMO molecular orbitals of the nanoparticle, changing its electrical conductivity, which is helpful for designing the novel sensor and remover devices. Charge analysis based on Mulliken charges reveals that charge is transferred from thiophene molecule to TiO<sub>2</sub> nanoparticle.

**Keywords:** Thiophene; TiO<sub>2</sub>; Electronic properties; Density functional theory.

### How to cite this article

Abbasi A, Jahanbin Sardroodi J. Van der Waals corrected DFT study on the adsorption behaviors of TiO<sub>2</sub> anatase nanoparticles as potential molecule sensor for thiophene detection. *J. Water Environ. Nanotechnol.*, 2017; 2(1): 52-65. DOI: 10.7508/jwent.2017.01.007

## INTRODUCTION

Titanium dioxide (TiO<sub>2</sub>) has been characterized as a most widely used photocatalytic material, which has various applications in photo-catalysis [1], gas sensor devices, heterogeneous catalysis [2] and photovoltaic cells [3]. Owing to some outstanding properties such as non-toxicity, chemical stability, abundance and high catalytic efficiency, it has attracted numerous scientific attentions in the recent years. These unique properties of TiO<sub>2</sub> make it very interesting material to be utilized in many fields of science and research [4-8]. Numerous attempts have been done to cover all theoretical aspects of TiO<sub>2</sub> related science and

technology including fundamental principles and crucial practical features of it [8-15]. The photocatalytic activity of TiO<sub>2</sub> has been restricted due to its relatively wide band gap, which decreases the absorption of the incoming solar irradiation. One convenient solution to enhance the optical response of TiO<sub>2</sub> is the doping of TiO<sub>2</sub> with some non-metal elements such as nitrogen [16-18]. Several computational studies of N-doped TiO<sub>2</sub> nanoparticles have been suggested by different researchers. For example, Liu *et al.* reported that the N doping can facilitate the adsorption of nitric oxide on TiO<sub>2</sub> anatase nanoparticles [14]. Recently, it has been revealed that the N-doped TiO<sub>2</sub>

\* Corresponding Author Email: [a\\_abbasi@azaruniv.edu](mailto:a_abbasi@azaruniv.edu)

anatase nanoparticles react with CO molecules more efficiently, compared to the undoped ones [19]. Moreover, the nitrogen doping of TiO<sub>2</sub> nanoparticles makes it possible to apply TiO<sub>2</sub> as an efficient sensor material, altering its electronic and structural properties [20-25]. Nevertheless, the impacts of N-doping on the photo-catalytic activity and therefore the energy gap of TiO<sub>2</sub> have been inspected in some other works [26, 27]. In order to reveal the enhancement of the efficiency of TiO<sub>2</sub> nanoparticles in the adsorption processes some researchers have analyzed its electronic properties such as density of states (DOS), Mulliken population analysis and also its structural properties such as bond lengths and adsorption energies [14, 19, 28]. A material in the atmosphere which causes harmful effects on the public health and the environment is identified as an air pollutant, which can have different forms such as solid particles, liquid droplets or gasses. Thiophene is a heterocyclic compound and is one of the main constituents of fuel. The combustion of thiophene molecule leads to the production of sulfur containing compounds, which are characterized as harmful materials and can participate to the environmental pollution. Since environment protection is a serious subject to the public health, the concentration of sulfur is severely controlled by using the appropriate methods. Hence, the removal of sulfur from sulfur containing compounds especially thiophene is a major point, which facilitates the production of clean fuels with low content of sulfur atom [29-32]. An admirable gas sensor should have high sensitivity to the anticipated poisonous material, as well as extensive variety of application and low price fabrication. Solid state sensors such as TiO<sub>2</sub> anatase nanoparticles are well-known and broadly used materials for recognition of harmful molecules in the atmosphere due to their unique response to the air pollutants. It has been mentioned that the N-doped TiO<sub>2</sub> can be classified as an efficient candidate for detecting different molecules. In this research, we studied the sensitivity of both undoped and N-doped TiO<sub>2</sub> anatase nanoparticles for interaction with harmful thiophene molecule. We provided various adsorption configurations of the thiophene with respect to the nanoparticles. The adsorption energies, electronic properties including the total and projected density of states, the structural properties and the charge transfer analysis of the considered non-adsorbed and adsorbed structures in adsorbed complexes were

computed and analyzed. It can be concluded that the electronic properties of TiO<sub>2</sub> anatase nanoparticle, are strongly changed by the adsorption of thiophene. This work is devoted to supply a theoretical basis for the design and manufacture of effective TiO<sub>2</sub> based sensor devices for thiophene detection.

## COMPUTATIONAL DETAILS AND MODELS

### Computational Methods

Density Functional Theory (DFT) calculations [33, 34] were carried out using the Open source Package for Material eXplorer (OPENMX) ver. 3.8 [35], being a well-organized software package for nano-scale materials simulations based on DFT, PAO basis functions and VPS pseudopotentials. Pseudo atomic orbitals were utilized as basis sets in the geometry optimizations. The considered cutoff energy was set to the value of 150 Rydberg in our calculations [34]. The PAO's were constructed through the basis sets (3-s, 3-p, 1-d) for the titanium atom, (2-s and 2-p) for the oxygen, carbon and nitrogen atoms, (2-s) for the hydrogen atom and (3-s and 3-p) for the sulfur atom with the chosen cutoff radii of 7 for the titanium, 5 for the oxygen, carbon, nitrogen and hydrogen atoms and 8 for sulfur atom (all in bohrs). The exchange-correlation energy functional was described using the generalized gradient approximation (GGA) in the Perdew–Burke–Ernzerhof form (PBE) [36]. The van der Waals interactions were examined using the DFT-D2 method. The convergence criteria for self-consistent field iterations and energy calculation were set to the values of  $1.0 \times 10^{-6}$  Hartree and  $1.0 \times 10^{-4}$  Hartree/bohr, respectively. For the geometry optimization, 'Opt' is used as the geometry optimizer, which is a robust and efficient scheme. The crystalline and molecular structure visualization program, XCrysDen [37], was employed for displaying molecular orbital isosurfaces. The Gaussian broadening method for evaluating electronic DOS was used. For the adsorption of thiophene molecules on the TiO<sub>2</sub>/MoS<sub>2</sub> nanocomposite. The adsorption energy was calculated by using the following formula:

$$E_{ad} = E_{(particle + adsorbate)} - E_{particle} - E_{adsorbate} \quad (1)$$

where  $E_{(particle + adsorbate)}$ ,  $E_{particle}$  and  $E_{adsorbate}$  are the energies of the complex system, the free TiO<sub>2</sub> nanoparticle without any adsorbed molecule and the free thiophene molecule in a non-adsorbed state respectively. The charge transfer between the thiophene molecule and the nanoparticles

was evaluated using the Mulliken charge analysis, which is based on the difference of the charge concentration on thiophene before and after the adsorption process.

#### Modelling of nanoparticles

We have constructed the TiO<sub>2</sub> anatase nanoparticles by setting a 3×2×1 supercell of pristine and N-doped TiO<sub>2</sub> anatase. The considered unit cell of TiO<sub>2</sub> was reported by Wyckoff [38], which was chosen from “American Mineralogists Database” webpage [39]. The chosen supercell of TiO<sub>2</sub> anatase was shown in Fig. 1. The size of the

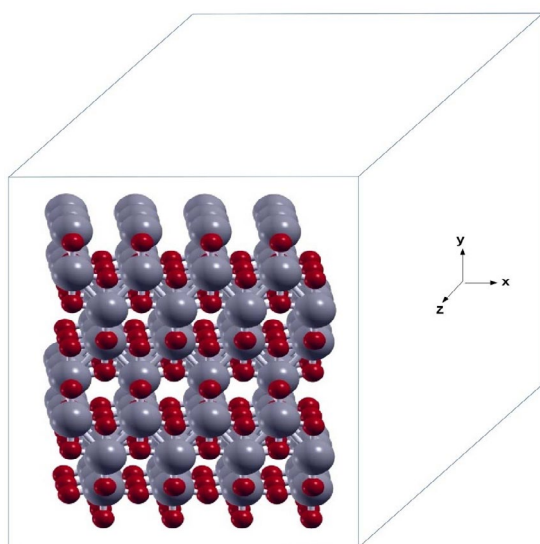


Fig. 1. Representation of a 3×2×1 supercell of TiO<sub>2</sub> anatase constructed from TiO<sub>2</sub> unit cells along x, y and z directions.

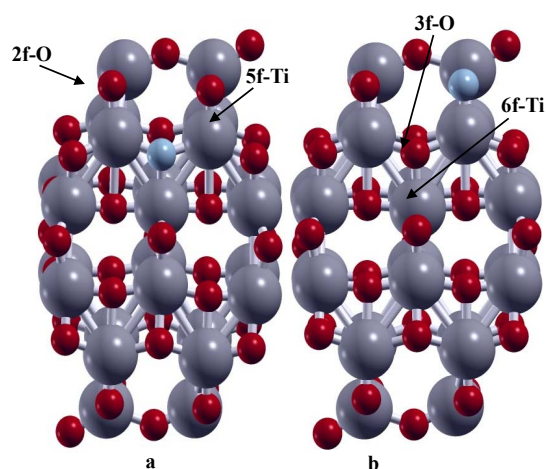


Fig. 2. Optimized N-doped TiO<sub>2</sub> anatase nanoparticles constructed using the 3×2×1 unit cells, colors represent atoms accordingly: Ti in gray, O in red and N in blue.

simulation box considered in our calculations is 20×15×30 Å<sup>3</sup>, being much larger than the nanoparticle size. A vacuum space of 11.5 Å was set between neighbor particles to avoid the additional interactions between repeated slabs. Two oxygen atoms of pristine TiO<sub>2</sub> (twofold coordinated and threefold coordinated oxygen atoms) were substituted by nitrogen atoms to prepare N-doped nanoparticles. Twofold coordinated oxygen atom is denoted by 2f-O and threefold by 3f-O (middle oxygen) in Fig. 2 with fivefold coordinated and sixfold coordinated titanium atoms sketched by 5f-Ti and 6f-Ti, respectively [40]. The schematic structures of thiophene molecule is represented in Fig. 3. The thiophene molecule is positioned in parallel and perpendicular geometries with respect to the optimized undoped and N-doped nanoparticles. The complex system optimization reveals that the sulfur atom of thiophene molecule preferentially interacts with fivefold coordinated titanium atom of nanoparticle and is close to the surface titanium site. It means a higher activity of sulfur atom of thiophene, compared to the other atoms.

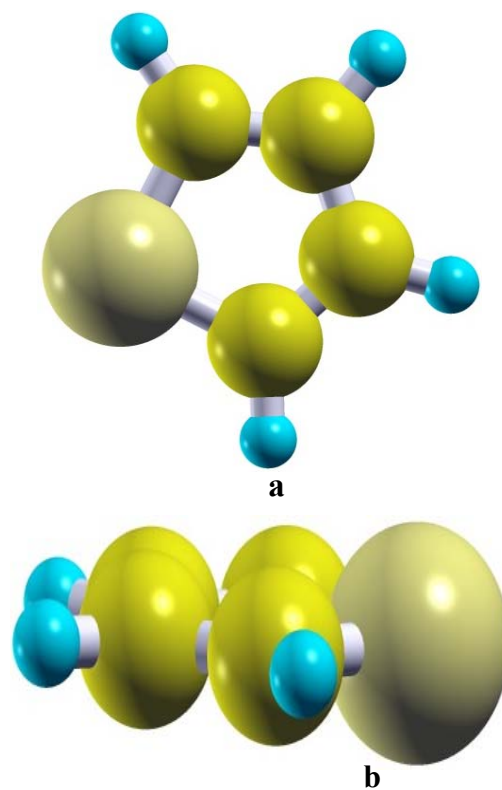


Fig. 3. Representation of the optimized structure of thiophene molecule, (a): front view and (b): lateral view. Colors represent atoms accordingly: S in light yellow, C in dark yellow and H in cyan.

## RESULTS AND DISCUSSION

### Structure parameters and adsorption energies

According to the structure of thiophene, the thiophene molecule was adsorbed on the fivefold coordinated titanium site of TiO<sub>2</sub> nanoparticles in two possible adsorption geometries. In one geometry, the thiophene molecule was placed vertically (perpendicular geometry) towards the nanoparticle and the other is that thiophene was put horizontally (parallel geometry). Adsorption geometries of thiophene molecule on the optimized TiO<sub>2</sub> nanoparticle are displayed in Fig. 4. This Figure includes the thiophene-adsorbed complexes named A-I for the perpendicular and parallel configurations. Each complex of Fig. 4 differs in substituted oxygen atom of TiO<sub>2</sub> nanoparticle and the relative orientation of thiophene molecule with respect to the nanoparticle from the others. For example, complex A tells the

perpendicular orientation of thiophene towards the O<sub>C</sub>-substituted nanoparticle. The optimized values of some bond lengths before and after the adsorption on the nanoparticle were listed in Table 1. The bond lengths include the newly formed Ti-S bond, T-O bond and C-S bond of thiophene molecule. The results indicate that the C-S bond of thiophene molecule and Ti-O bonds of TiO<sub>2</sub> nanoparticle are stretched after the adsorption process. These elongations in the bond lengths are mostly attributed to the transfer of electronic density from Ti-O bond of TiO<sub>2</sub> and C-S bond of the adsorbed thiophene molecule to the newly formed Ti-S bond between TiO<sub>2</sub> nanoparticle and thiophene molecule. The smaller bond formed between the sulfur atom of thiophene molecule and the titanium atom of nanoparticle (Ti-S), has stronger interaction between thiophene and TiO<sub>2</sub> anatase nanoparticle. Adsorption energy analysis

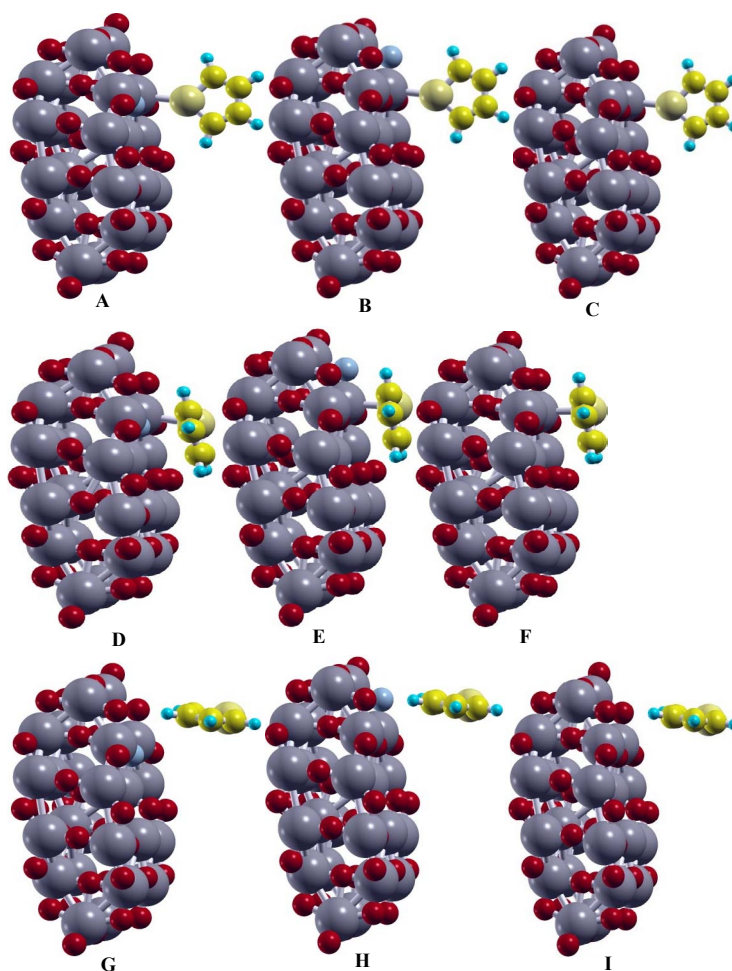


Fig. 4. Optimized geometry configurations of TiO<sub>2</sub> anatase nanoparticles with adsorbed thiophene molecule.

reveals that the thiophene molecule is preferentially adsorbed on the fivefold coordinated titanium site of nanoparticle through its sulfur atom rather than its carbon and hydrogen atoms. The bond lengths relevant to the perpendicular (H-site) configurations were also listed in Table 2. The adsorption energies of the most stable configurations were tabulated in Table 3. These results indicate that the adsorption of thiophene molecule on the N-doped nanoparticle is more energetically favorable than the adsorption on the undoped one. The higher adsorption energy and small adsorption distance indicate chemisorption of thiophene molecule on the nanoparticles. O<sub>C</sub>-substituted nanoparticle adsorbs the thiophene molecule more efficiently, compared to the O<sub>T</sub>-substituted one. Therefore, the N-doped nanoparticles have higher sensing capabilities than the pristine ones, suggesting that the N-doping strengthens the adsorption of thiophene on the TiO<sub>2</sub> nanoparticle. The

more negative the adsorption energy, the higher tendency for adsorption, and consequently more stable adsorption geometry. As can be seen from Table 3, all the calculated adsorption energies are considerably increased when the vdW interactions are taken into account. Therefore, the adsorption energies of thiophene molecule on the undoped and nitrogen-doped TiO<sub>2</sub> nanoparticles becomes higher when the vdW interactions are included, suggesting the significant domination of vdW interactions during the adsorption process. The improvement of both adsorption energy and structural properties of the adsorption of thiophene on TiO<sub>2</sub> resulted from N-doping reveals that the N-doped TiO<sub>2</sub> can be successfully used for removal of the toxic thiophene molecules from the environment. The nitrogen doping effect on the improvement of the adsorption ability of TiO<sub>2</sub> nanoparticles for adsorption of CO molecule has been recently discussed by Liu *et al.* [19].

Table 1: Bond lengths (in Å) for a thiophene molecule adsorbed on the TiO<sub>2</sub> anatase nanoparticles.

Complex	Ti-N	Ti-O	Newly-formed Ti-S	C-S
Perpendicular	---	---	---	---
A	---	1.76	2.73	1.83
B	1.79	---	2.73	1.81
C	---	1.73	2.72	1.81
Parallel (S site)	---	---	---	---
D	---	1.74	2.82	1.85
E	1.79	---	2.72	1.82
F	---	1.73	2.76	1.82
Non-adsorbed	1.76	1.73	---	1.79

Table 2: Bond distances (in Å) for a thiophene molecule adsorbed on the TiO<sub>2</sub> anatase nanoparticles in perpendicular (H site) adsorption configuration.

Complex	O-H1	O-H2	N-H1	C-H1	C-H2	Ti-O	Ti-O	Ti-N
G	2.33	2.50	---	1.10	1.10	1.76	1.84	---
G	---	2.52	2.30	1.10	1.10	1.78	---	1.80
I	2.43	2.56	---	1.09	1.10	1.74	1.81	---
Non-adsorbed	---	---	---	1.04	1.04	1.73	1.73	1.76

Table 3: Adsorption energies (eV) and Mulliken charges (e) for a thiophene molecule adsorbed on the TiO<sub>2</sub> anatase nanoparticles.

Complex	Mulliken charge	Adsorption energy	
		PBE	DFT-D2
Perpendicular (S site)			
A	-0.448	-3.60	-9.20
B	-0.282	-3.06	-8.90
C	-0.214	-0.61	-3.80
Parallel (S site)			
D	-0.711	-4.24	-10.08
E	-0.452	-3.57	-9.60
F	-0.457	-1.17	-5.30
Perpendicular (H site)			
G	-0.145	-3.22	-9.45
H	-0.253	-2.85	-8.60
I	-0.033	-0.19	-3.10

*Electronic structures*

Fig. 5 displays the total density of states (TDOS) for the non-adsorbed thiophene molecule. This figure represents that the energy gap between the HOMO and the LUMO levels is about 3.8 eV for the thiophene molecule. The TDOS of the complex systems containing TiO<sub>2</sub>+Thiophene couples were displayed in Fig. 6 and 7, which shows that the differences between DOS of doped and undoped

TiO<sub>2</sub> are increased by adsorption of thiophene. These differences include both changes in the energies of the peaks and creation of some small peaks in the DOS of N-doped TiO<sub>2</sub> at the energy values ranging from -8 eV to -15 eV. So, these variations in DOS states would affect the electronic transport properties of the nanoparticles and this feature can be beneficial for sensing of thiophene by TiO<sub>2</sub> nanoparticles. The titanium and sulfur

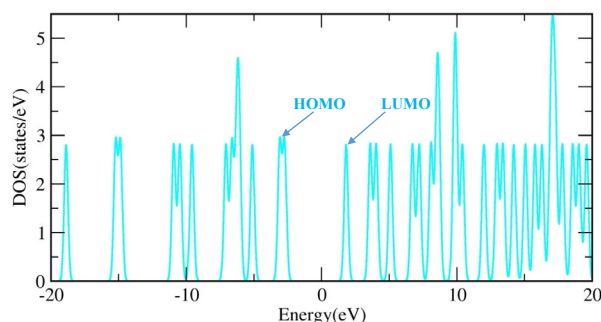


Fig. 5. Total density of states for thiophene molecule before the adsorption process.

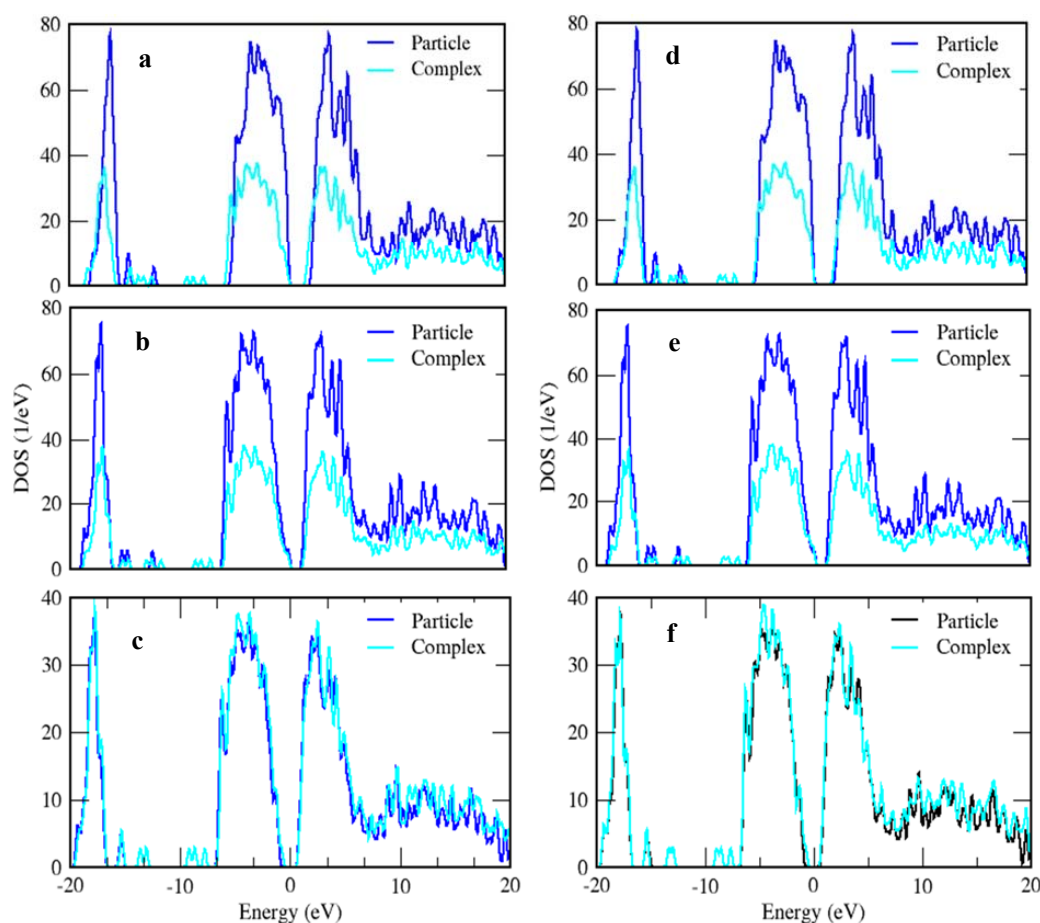


Fig. 6. Density of states for the adsorption of a thiophene molecule on the TiO<sub>2</sub> anatase particles, a: A complex; b: B complex; c: C complex; d: D complex; e: E complex; f: F complex.

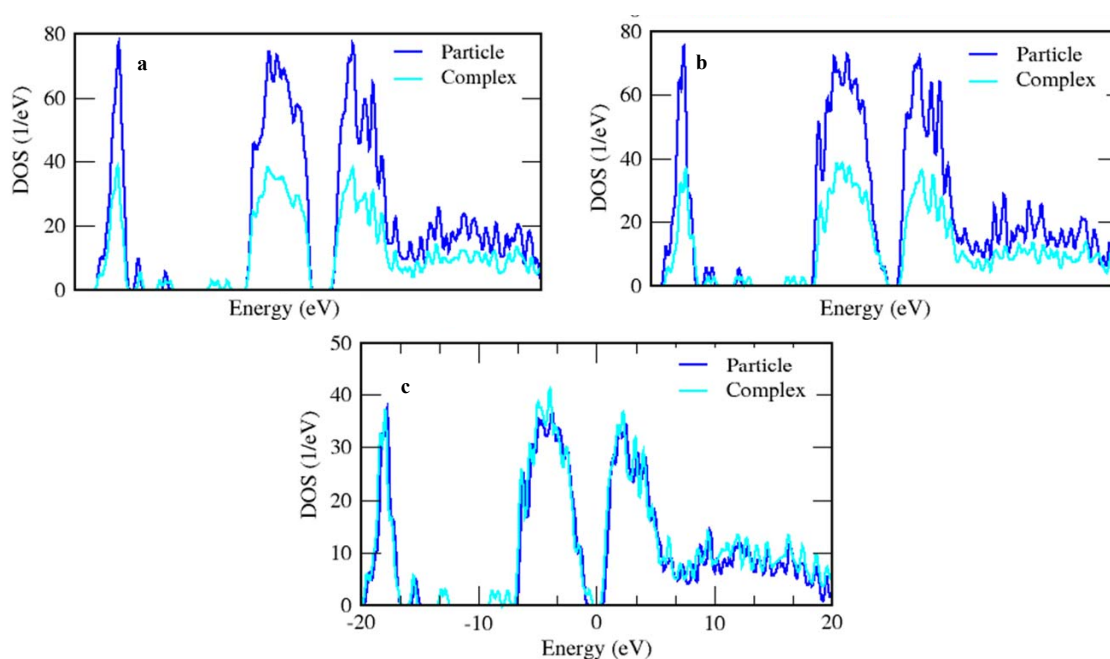


Fig. 7. Density of states for the adsorption of a thiophene molecule on the TiO<sub>2</sub> anatase particles, a: G complex; b: H complex; c: I complex.

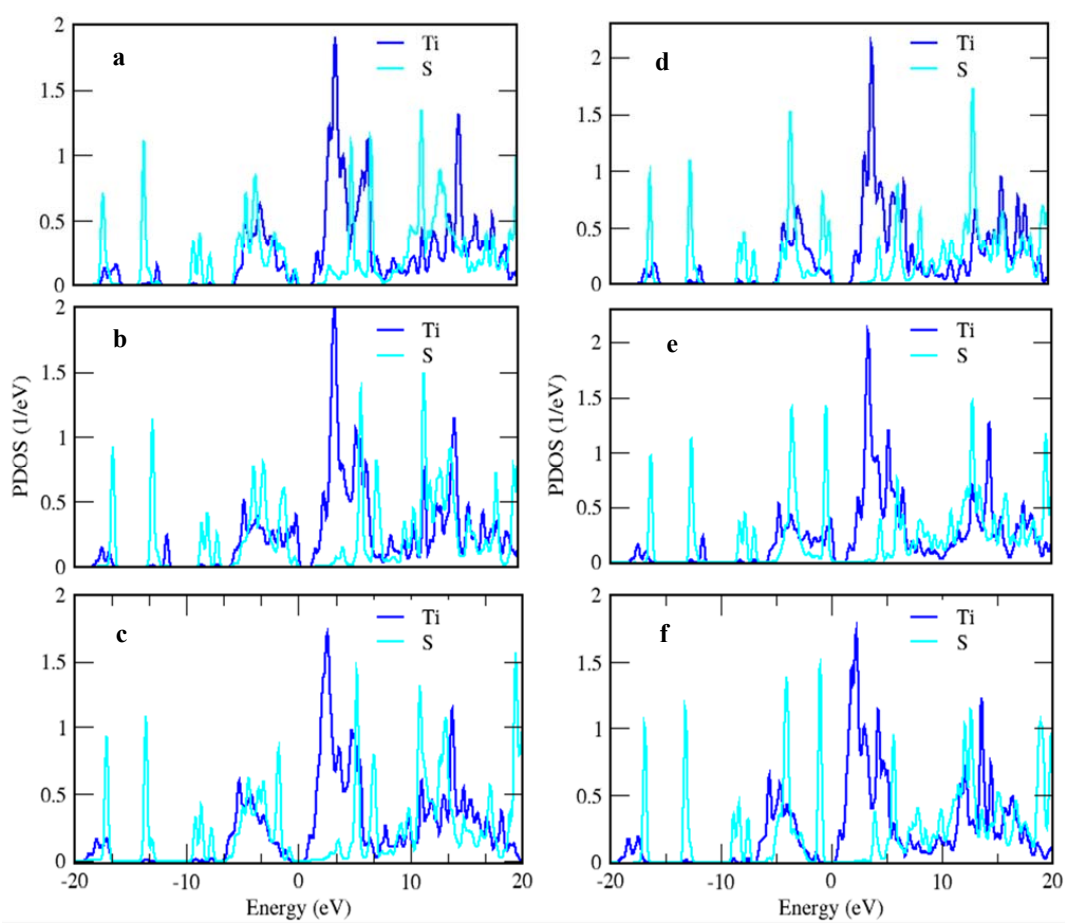


Fig. 8. Projected density of states for the adsorption of thiophene molecule on the TiO<sub>2</sub> anatase nanoparticles, a: A complex; b: B complex; c: C complex; d: D complex; e: E complex; f: F complex.

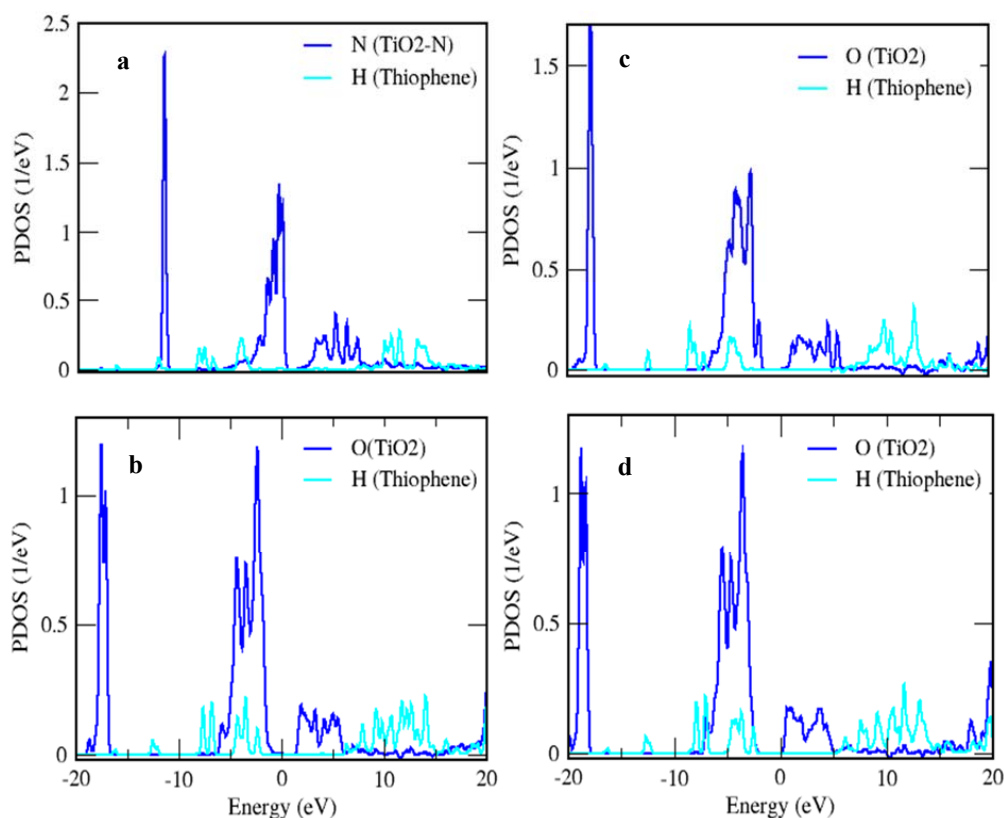


Fig. 9. Projected density of states for the adsorption of thiophene molecule on the TiO<sub>2</sub> anatase nanoparticles, a: H complex; b: H complex; c: G complex; d: G complex.

projected DOSs (Ti-PDOS and S-PDOS) for perpendicular and parallel (S site) configurations were shown in Fig. 8 as panels (a-f). The large overlap between the PDOSs of titanium and sulfur atoms reveals that the new Ti-S bond forms between the titanium atom of nanoparticle and sulfur atom of thiophene. The corresponding PDOSs for the perpendicular (H site) configuration were also shown in Fig. 9, which indicates a lower overlap between the PDOS of oxygen atoms of TiO<sub>2</sub> nanoparticle and hydrogen atoms of thiophene molecule. This implies that there is a weak mutual interaction between hydrogen atoms of thiophene and oxygen atoms of nanoparticle. The PDOSs of the titanium and sulfur atoms and their pertaining d orbitals were presented in Fig. 10 for complex A. This figure shows the highest overlap between the PDOSs of sulfur atom and d<sup>1</sup> orbital of titanium atom, compared with the other d orbitals. This is probably due to the higher contribution of d<sup>1</sup> orbital of titanium atom in chemical bond formation with sulfur atom. Fig. 11 contains the HOMO and LUMO orbitals of the thiophene molecule before the adsorption process. Interestingly, the

HOMO of thiophene is dominant at the middle of C-C and C-H bonds as shown in Fig. 11, whereas the electronic density in the LUMO of thiophene seem to be distributed over the whole thiophene molecule. Figs. 12 and 13 show the HOMO and LUMO molecular orbitals of the TiO<sub>2</sub> nanoparticles with adsorbed thiophene molecule, respectively. As shown in these figures, the HOMOs are strongly distributed over the thiophene molecule, whereas the LUMOs are dominant at the TiO<sub>2</sub> nanoparticle. The higher accumulation of the electronic density at the thiophene molecule depicted in the HOMO orbitals is a good electronic reason taken into account for the transfer of the electronic density from the thiophene molecule to the TiO<sub>2</sub> nanoparticle. Fig. 14 represents the spin polarized density of states of TiO<sub>2</sub>+Thiophene couples with the distribution of spin densities shown in Fig. 15. It can be seen that the magnetization is mainly located on the thiophene molecule. As a matter of convenience, we presented the spin polarized DOSs and plots for two complexes only. The difference electron densities measured from atomic density for the thiophene molecule adsorbed on

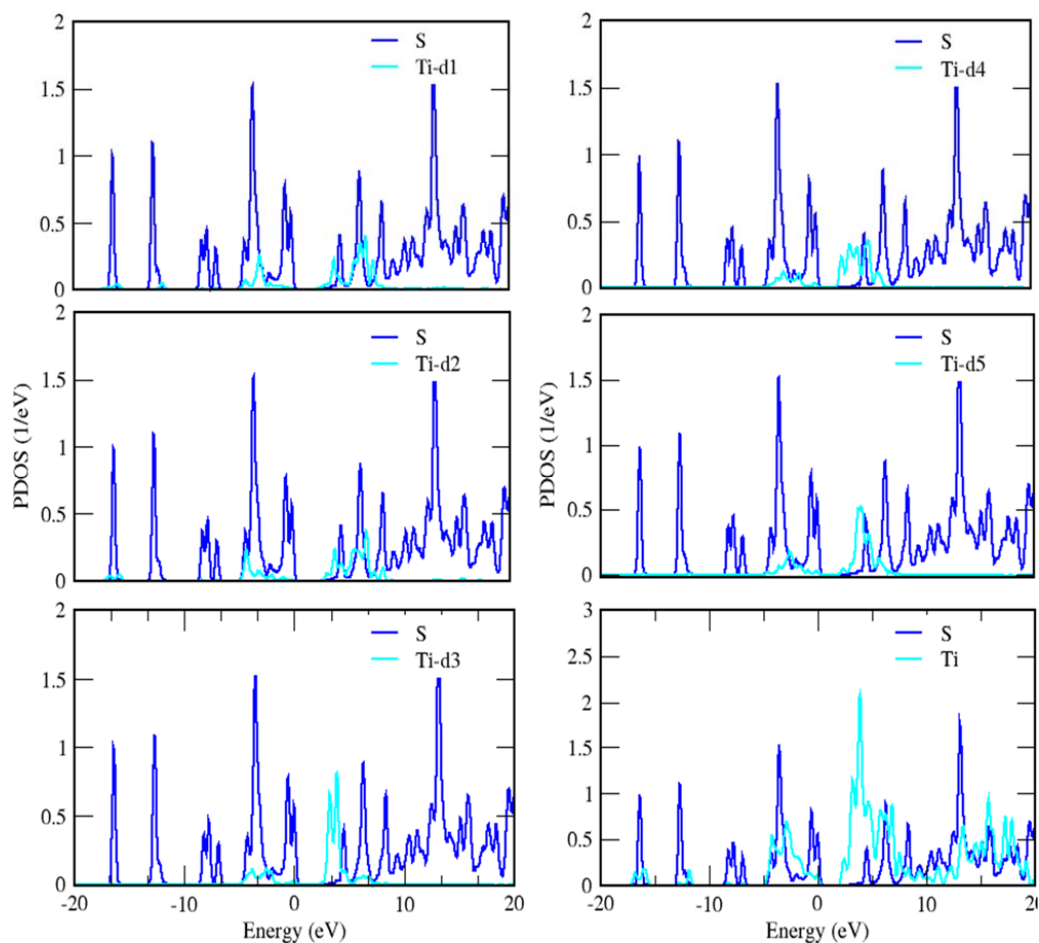


Fig. 10. Projected density of states for the sulfur atom of thiophene, titanium atom and different d orbitals of titanium.

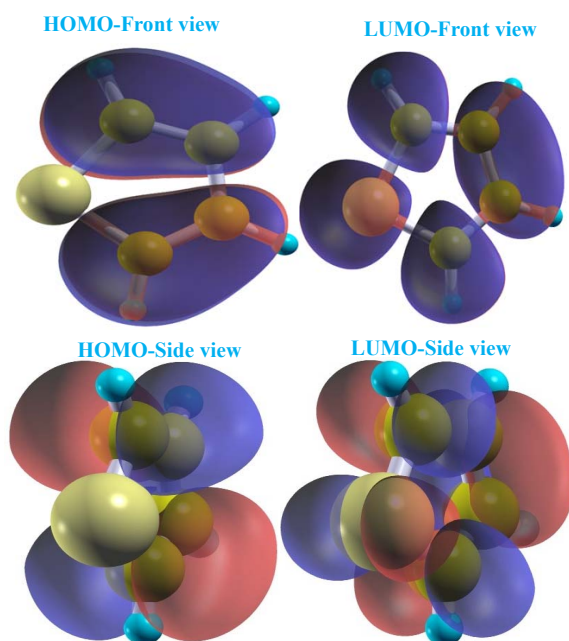
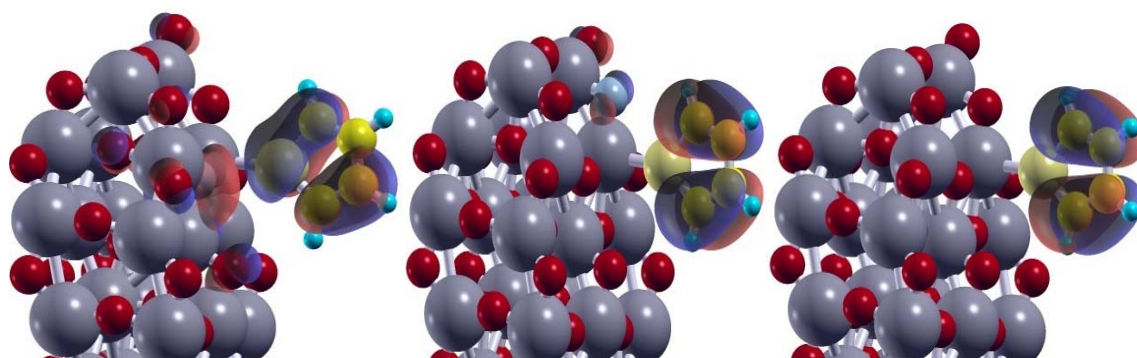
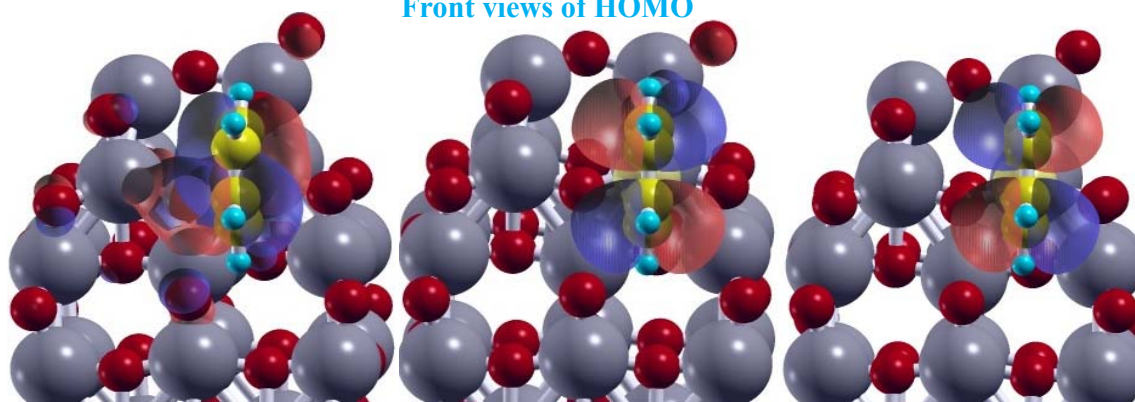


Fig. 11. HOMO and LUMO orbitals of a thiophene molecule in both front and side views.

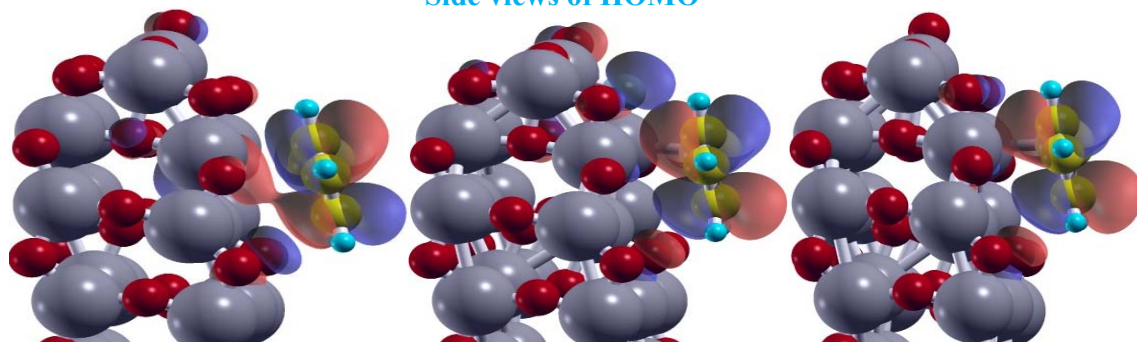
Side views of HOMO



Front views of HOMO



Side views of HOMO



Side views of HOMO

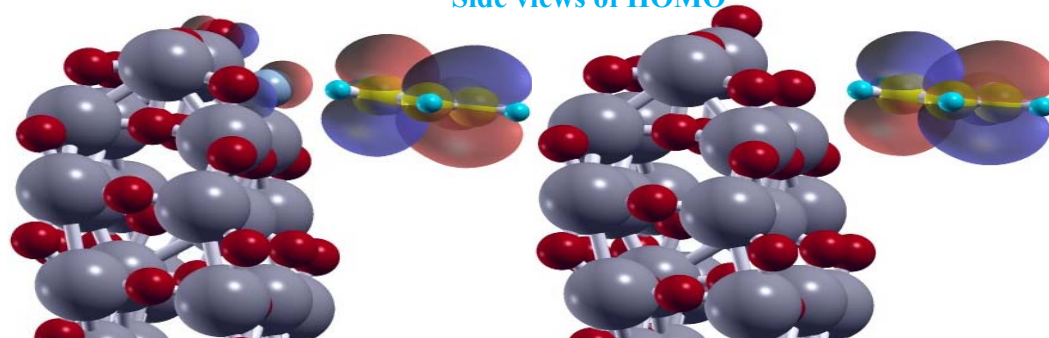


Fig. 12. The isosurfaces of HOMO molecular orbitals of thiophene molecule adsorbed on the considered nanoparticles.

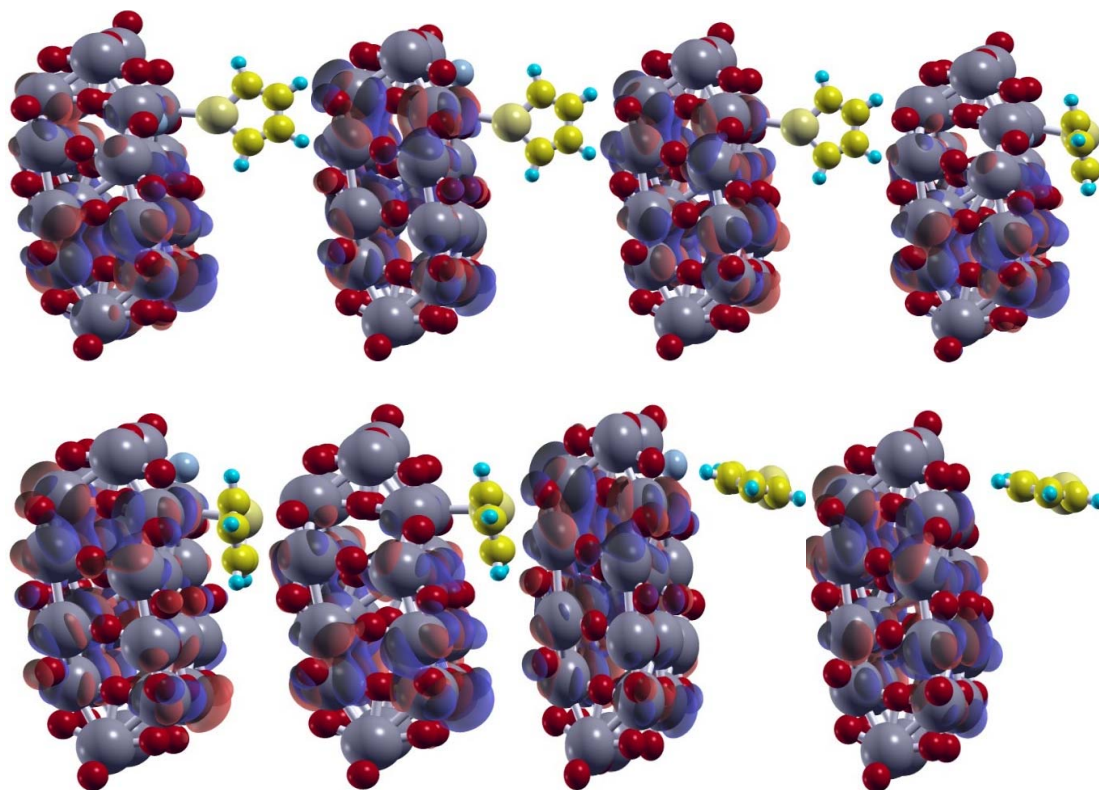


Fig. 13. The isosurfaces of LUMO molecular orbitals of thiophene molecule adsorbed on the considered nanoparticles

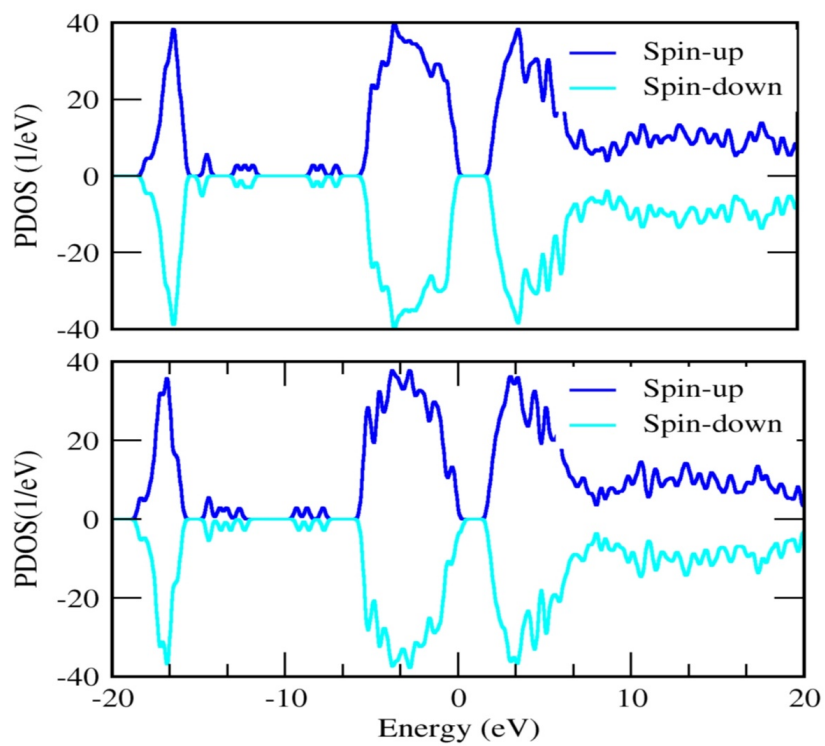


Fig. 14. Spin polarized density of states for the thiophene adsorption on the considered nanoparticles.

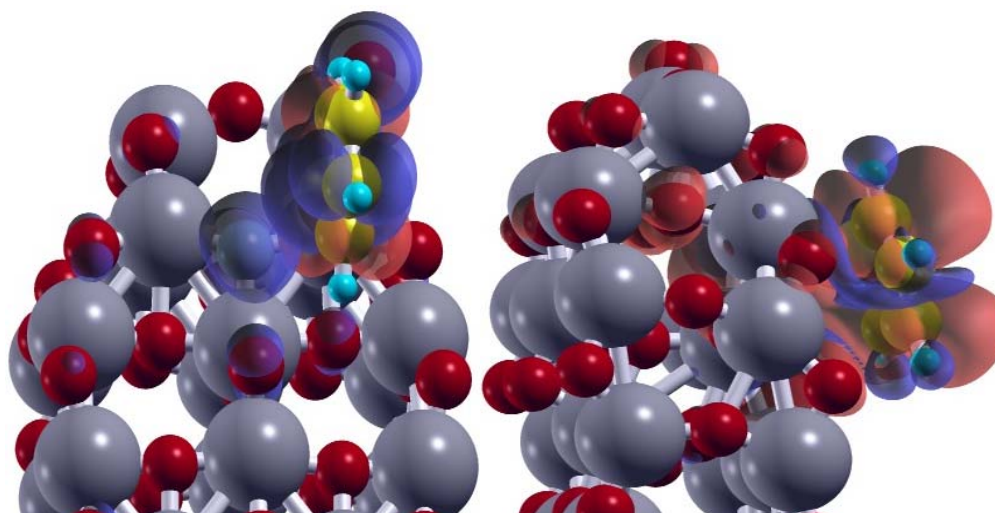


Fig. 15. Spin distribution density plots for the thiophene adsorption on the considered nanoparticles.

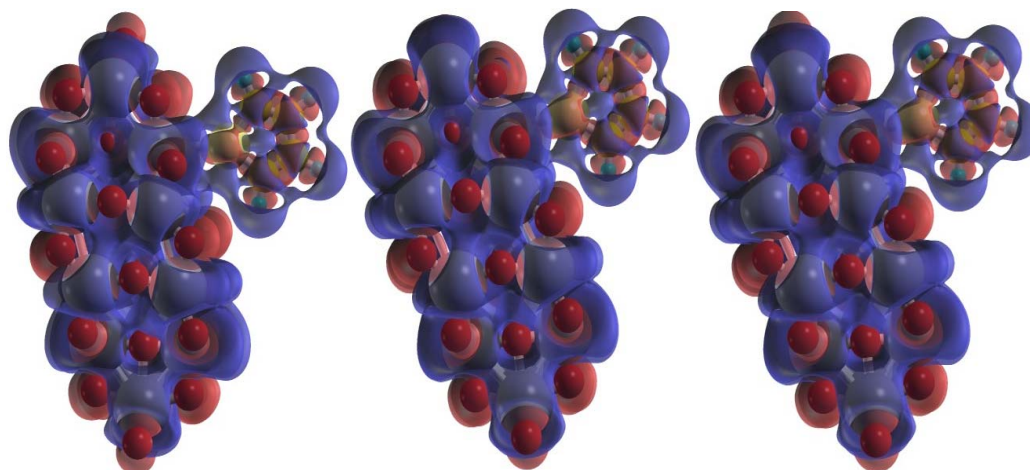


Fig. 16. The difference electron density measured from atomic density for the thiophene molecule adsorbed on the TiO<sub>2</sub> nanoparticles.

the TiO<sub>2</sub> nanoparticles were displayed in Fig. 16. This figure shows the electronic density both on the nanoparticle and the thiophene molecule for clear comparison between the densities. To further analyze the charge transfer between nanoparticle and thiophene molecule, we reported the Mulliken charge values in Table 3. Our analysis of the charge transfer results indicates that thiophene adsorption induces a significant charge transfer of about -0.448 e from thiophene to the TiO<sub>2</sub> nanoparticle for configuration A, suggesting the donor property of thiophene molecule in reaction with TiO<sub>2</sub> nanoparticle. This would be an effective property to help in the development of efficient sensor and remover devices for thiophene detection in the environment.

## CONCLUSIONS

In this letter, we have carried out density functional theory calculations on structural and electronic properties of undoped and N-doped TiO<sub>2</sub> anatase nanoparticles. The results reveal that the N-doped nanoparticles are more energetic than the undoped ones and can react with thiophene molecules more efficiently. With vdw interactions counted in calculations, it was found that the thiophene molecule is preferentially chemisorbed on the fivefold coordinated titanium site of TiO<sub>2</sub> nanoparticle. Parallel (S site) adsorption geometries are more stable than the perpendicular ones. The order of adsorption energy is calculated to be Parallel(S site) > Perpendicular(S

site) > Perpendicular (H site). We have also commented on the electronic properties of the studied systems including the DOS and molecular orbital plots in order to understand the electron transport phenomena. The obtained results indicate that the N-doped anatase nanoparticles are more active than the undoped ones. The N doping yields an increased affinity for TiO<sub>2</sub> nanoparticles to interact with thiophene molecules in the environment, being an efficient property to be utilized in sensing and removing applications. Our calculated results thus suggest a theoretical basis for the N-doped TiO<sub>2</sub> nanoparticles to be effectively employed in manufacturing the efficient sensor devices for thiophene recognition in the environment.

#### ACKNOWLEDGEMENT

This work has been supported by Azarbaijan Shahid Madani University.

#### CONFLICT OF INTEREST

The authors declare that there are no conflicts of interest regarding the publication of this manuscript.

#### REFERENCES

- Diebold, U. The surface science of titanium dioxide. *Surf. Sci. Reports*, **48**, 53-229 (2003).
- Han, F., Kambala, V. S. R., Srinivasan, M., Rajarathnam, D., Naidu, R. J. *Applied Catalysis A: General*, **2009**, 359, 25-40.
- Fujishima, A.; Honda, K. *Electrochemical Photolysis of Water at a Semiconductor Electrode Nature*. **238**, 37 (1972).
- Linsebigler, A. L.; Lu, G.; Yates, J. T. *Photocatalysis on TiO<sub>2</sub> Surfaces: Principles, Mechanisms, and Selected Results*, *J. Chem. Rev.* **95**(3), 735 (1995).
- Zhang, C.; Lindan, P. J. D. A density functional theory study of sulphur dioxide adsorption on rutile TiO<sub>2</sub> (1 1 0), *J. Chemical Physics Letters* **373**, 15-21, (2003).
- Erdogan, R.; Ozbek, O.; Onal, I. A periodic DFT study of water and ammonia adsorption on anatase TiO<sub>2</sub> (001) slab, *J Surf Sci.* **604**, 1029-1033, (2010).
- Hummatov, R.; Gulseren, O.; Ozensoy, E.; Toffoli, D.; Ustunel, H. First-Principles investigation of NO<sub>x</sub> and SO<sub>x</sub> adsorption on anatase supported BaO and Pt overlayers, *J Phys Chem C* **116**, 6191-6199, (2012).
- Fahmi, A.; Minot, C. A theoretical investigation of water-adsorption on titanium dioxide surfaces, *Surf. Sci.* **304**, 343-359, (1994).
- Onal, I.; Soyer, S.; Senkan, S. Adsorption of water and ammonia on TiO<sub>2</sub>-anatase cluster models *J. Surface Science*, **600**, 2457-2469 (2006).
- Shi, W.; Chen, Q.; Xu, Y.; Wu, D.; Huo, C. F. Investigation of the silicon concentration effect on Si-doped anatase TiO<sub>2</sub> by first-principles calculation, *Journal of Solid State Chemistry*. **184**(8), 1983 (2011).
- Lei, Y.; Liu, H.; Xiao, W. First principles study of the size effect of TiO<sub>2</sub> anatase nanoparticles in dye-sensitized solar cell, *Modelling Simul. Mater. Sci. Eng.* **18**, 025004 (2010).
- Beltran, A.; Andres, J.; Sambrano, J. R.; Longo, E. Density Functional Theory Study on the Structural and Electronic Properties of Low Index Rutile Surfaces for TiO<sub>2</sub>/SnO<sub>2</sub>/TiO<sub>2</sub> and SnO<sub>2</sub>/TiO<sub>2</sub>/SnO<sub>2</sub> Composite Systems, *The Journal of Physical Chemistry A*. **112**(38), 8943. (2008).
- Tang, S.; Cao, Z. Adsorption of nitrogen oxides on graphene and graphene oxides: Insights from density functional calculations, *J. Chem. Phys.* **134**, 044710 (2011).
- Liu, J.; Liu, Q.; Fang, P.; Pan, C.; Xiao, W. First principles study of the adsorption of a NO molecule on N-doped anatase nanoparticles, *J Appl. Surf. Sci.* **258**, 8312-8318, (2012).
- Abbasi, A.; Sardroodi, J. J.; Ebrahimzadeh, A. R. Improving the adsorption of sulphur trioxide on TiO<sub>2</sub> anatase nanoparticles by N-doping: A DFT study, *Journal of Theoretical and Computational Chemistry*. **14**(4), 1550025 (1-24) (2015).
- Irie, H.; Watanabe, Y.; Hashimoto, K. Nitrogen-Concentration Dependence on Photocatalytic Activity of TiO<sub>2-x</sub>N<sub>x</sub> Powders, *Journal of Physical Chemistry B* **107**(23), 5483-5486, (2003).
- Tang, S.; Zhu, J. Structural and electronic properties of Pd decorated graphene oxides and their effects on the adsorption of nitrogen oxides: insights from density functional calculations, *J. RSC Adv.* **4**, 23084 (2014).
- Chen, Q.; Tang, C.; Zheng, G. First-principles study of TiO<sub>2</sub> anatase (101) surfaces doped with N, *Physica B: Condens. Matter*, **404**:1074-1078, 2009.
- Liu, J.; Dong, L.; Guo, W.; Liang, T.; Lai, W. CO adsorption and oxidation on N-doped TiO<sub>2</sub> nanoparticles, *J. Phys. Chem. C*. **117**, 13037, (2013).
- Abbasi, A.; Sardroodi, J. J.; Ebrahimzadeh, A. R. The adsorption of SO<sub>2</sub> on TiO<sub>2</sub> anatase nanoparticles: A density functional theory study, *Can. J. Chem.* **94**(1), 78-87 (2016).
- Livraghi, S.; Paganini, M. C.; Giamello, E.; Selloni, A.; Valentin, C. D.; Pacchioni, G. Origin of Photoactivity of Nitrogen-Doped Titanium Dioxide under Visible Light, *Journal of the American Chemical Society* **128**(49), 15666-15671, (2006).
- Liu, H.; Zhao, M.; Lei, Y.; Pan, C.; Xiao, W. Formaldehyde on TiO<sub>2</sub> anatase (1 0 1): A DFT study, *J Comput Mater Sci.* **15**, 389-395, (2012).
- Breedon, M.; Spencer, M.; Yarovsky, I. Adsorption of NO<sub>2</sub> on Oxygen Deficient ZnO (21-1-0) for Gas Sensing Applications: A DFT Study, *The Journal of Physical Chemistry C*. **114** (39), 16603 (2010).
- Rumaiz, A. K.; Woicik, J. C.; Cockayne, E.; Lin, H. Y.; Jaffari, G. H.; Shah, S. I. Oxygen vacancies in N doped anatase TiO<sub>2</sub>: Experiment and first-principles calculations, *Applied Physics Letters*. **95** (26), 262111 (2009).
- Zhao, Z.; Liu, Q. Effects of lanthanide doping on electronic structures and optical properties of anatase TiO<sub>2</sub> from density functional theory calculations, *Journal of Physics D: Applied Physics*, **41**(8), 085417 (2008).
- Gao, H.; Zhou, J.; Dai, D.; Qu, Y. Photocatalytic Activity and Electronic Structure Analysis of N-doped Anatase TiO<sub>2</sub>: A Combined Experimental and Theoretical Study, *J. Chem. Eng. Technol.* **32**, 867. (2009).
- Zhao, D.; Huang, X.; Tian, B.; Zhou, S.; Li, Y.; Du, Z. The effect of electronegative difference on the electronic structure and visible light photocatalytic activity of N-doped anatase TiO<sub>2</sub> by first-principles calculations, *Appl. Phys. Lett.* **98**, 115-124 (2011).

28. Landmann, M.; Rauls, E.; Schmidt, W. G. The electronic structure and optical response of rutile, anatase and brookite TiO<sub>2</sub>, *Journal of Physics: Condensed Matter* **24** 195503 (2012).
29. Parola, V. L.; Testa, M. L.; Venezia, A. M. Pd and PdAu catalysts supported over 3-MPTES grafted HMS used in the HDS of thiophene, *J. Appl. Catal. B. Environ.* **119**, 248-255 (2012).
30. Larminie, J.; Dicks, A. *Fuel Cell Systems Explained*, John Wiley, New York, (2000).
31. Urban, S.; Beiring, B.; Ortega, N.; Paul, D.; Glorius, F. Asymmetric Hydrogenation of Thiophenes and Benzothiophene, *J. Am. Chem. Soc.* **134**, 15241-15244 (2012).
32. Zhang, B. Y.; Jiang, Z. X.; Li, J.; Zhang, Y. N.; Lin, F.; Liu, Y.; Li, C. Catalytic oxidation of thiophene and its derivatives via dual activation for ultra-deep desulfurization of fuels. *J. Catal.* **287**, 5-12 (2012).
33. Hohenberg, P.; Kohn, W. Inhomogeneous electron gas, *J. Phys. Rev.* **136**, B864-871 (1964).
34. Kohn, W.; Sham, L. Self-Consistent equations including exchange and correlation effects, *Phys Rev*, **140**, A1133-A1138, (1965).
35. The code, OPENMX, pseudoatomic basis functions, and pseudopotentials are available on a web site '<http://www.openmxsquare.org>'.
36. Perdew, J. P.; Burke, K.; Ernzerhof, M. Generalized gradient approximation made simple, *J Phys Rev Lett.* **78**, 1396 (1997).
37. Koklj, A. Computer graphics and graphical user interfaces as tools in simulations of matter at the atomic scale, *J. Comput. Mater. Sci.* **28**, 155-168 (2003).
38. Wyckoff, R. W. G. *crystal structures*, Second edition. Interscience Publishers, USA, New York, **1963**.
39. Web page at: <http://rruff.geo.arizona.edu/AMS/amcsd>.
40. Wu, C.; Chen, M.; Skelton, A. A.; Cummings, P. T.; Zheng, T. *ACS Appl. Mat. Interfaces.* **2013**, 5, 2567-2579.